Research Article | Vol. 26, No. 2 | 22 Jan 2018 | OPTICS EXPRESS A136
Optics EXPRESS

Tuning the correlated color temperature of white light-emitting diodes resembling Planckian locus

ZIQIAN HE, HAIWEI CHEN, YUN-HAN LEE, AND SHIN-TSON WU*

College of Optics and Photonics, University of Central Florida, Orlando, FL 32816, USA
**swu@ucf.edu*

Abstract: We report a new electrically tunable color filter to actively adjust the correlated color temperature of white light-emitting diodes. With four passive cholesteric films and an active polarization rotator, both circular polarizations of the incident light are utilized to generate complementary blue and yellow colors. The blue/yellow ratio can be tuned by the applied voltage of the polarization rotator. In experiment, the tunable color filter offers a reasonably wide tuning range (1900 K and 2400 K), which resembles the Planckian locus. This design is promising for next generation smart lighting.

OCIS codes: (220.2945) Illumination design; (330.1690) Color; (230.3670) Light-emitting diodes; (230.3720) Liquid-crystal devices.

References and links

1. S. Nakamura, T. Mukai, and M. Senoh, "High-power GaN pn junction blue-light-emitting diodes," Jpn. J. Appl. Phys. **30**(2), L1998–L2001 (1991).
2. S. Nakamura, T. Mukai, and M. Senoh, "Candela-class high-brightness InGaN/AlGaN double-heterostructure blue-light-emitting diodes," Appl. Phys. Lett. **64**(13), 1687–1689 (1994).
3. S. Nakamura, "The roles of structural imperfections in InGaN-based blue light-emitting diodes and laser diodes," Science **281**(5379), 956–961 (1998).
4. E. F. Schubert and J. K. Kim, "Solid-state light sources getting smart," Science **308**(5726), 1274–1278 (2005).
5. J. Y. Tsao, M. H. Crawford, M. E. Coltrin, A. J. Fischer, D. D. Koleske, G. S. Subramania, G. T. Wang, J. J. Wierer, and R. F. Karlicek, Jr., "Toward smart and ultra-efficient solid-state lighting," Adv. Opt. Mater. **2**(9), 809–836 (2014).
6. P. R. Boyce, *Human Factors in Lighting*, 2nd ed. (Taylor & Francis, 2003).
7. "Osram Opto unveils brilliant-mix LED mixing concept," LEDs Mag., May 2011. *http://www.ledsmagazine.com/articles/2011/05/osram-opto-unveils-brilliant-mix-led-mixing-concept.html*.
8. S. Muthu, F. J. P. Schuurmans, and M. D. Pashley, "Red, green, and blue LEDs for white light illumination," IEEE J. Sel. Top. Quantum Electron. **8**(2), 333–338 (2002).
9. A. Zukauskas, R. Vaicekauskas, F. Ivanauskas, G. Kurilcik, Z. Bliznikas, K. Breive, J. Krupic, A. Rupsys, A. Novickovas, P. Vitta, A. Navickas, V. Raskauskas, M. S. Shur, and R. Gaska, "Quadrichromatic white solid-state lamp with digital feedback," Proc. SPIE **5187**, 185–198 (2004).
10. J. Y. Tsao, I. Brener, D. F. Kelley, and S. K. Lyo, "Quantum-dot-based solid-state lighting with electric-field-tunable chromaticity," J. Disp. Technol. **9**(6), 419–426 (2013).
11. W. Yang, P. Zhong, S. Mei, Q. Chen, W. Zhang, J. Zhu, R. Guo, and G. He, "Photometric optimization of color temperature tunable quantum dots converted white LEDs for excellent color rendition," IEEE Photonics J. **8**(5), 1–11 (2016).
12. C.-C. Huang, Y.-Y. Kuo, S.-H. Chen, W.-T. Chen, and C.-Y. Chao, "Liquid-crystal-modulated correlated color temperature tunable light-emitting diode with highly accurate regulation," Opt. Express **23**(3), A149–A156 (2015).
13. H. Chen, Z. Luo, R. Zhu, Q. Hong, and S. T. Wu, "Tuning the correlated color temperature of white LED with a guest-host liquid crystal," Opt. Express **23**(10), 13060–13068 (2015).
14. H. Chen, R. Zhu, Y.-H. Lee, and S.-T. Wu, "Correlated color temperature tunable white LED with a dynamic color filter," Opt. Express **24**(6), A731–A739 (2016).
15. S. A. Empedocles and M. G. Bawendi, "Quantum-confined stark effect in single CdSe nanocrystallite quantum dots," Science **278**(5346), 2114–2117 (1997).
16. L. I. Gurinovich, A. A. Lyutich, A. P. Stupak, M. V. Artem'ev, and S. V. Gaponenko, "Effect of an electric field on photoluminescence of cadmium selenide nanocrystals," J. Appl. Spectrosc. **77**(1), 120–125 (2010).
17. L. I. Gurinovich, A. A. Lutich, A. P. Stupak, S. Y. Prislopsky, E. K. Rusakov, M. V. Artemyev, S. V. Gaponenko, and H. V. Demir, "Luminescence in quantum-confined cadmium selenide nanocrystals and nanorods in external electric fields," Semiconductors **43**(8), 1008–1016 (2009).

#314847 https://doi.org/10.1364/OE.26.00A136
Journal © 2018 Received 4 Dec 2017; revised 21 Dec 2017; accepted 21 Dec 2017; published 4 Jan 2018

Optics EXPRESS

18. D. K. Yang and S. T. Wu, *Fundamentals of Liquid Crystal Devices,* 2nd ed. (John Wiley & Sons, 2014).
19. N. Tamaoki, "Cholesteric liquid crystals for color information technology," Adv. Mater. **13**(15), 1135–1147 (2001).
20. S. V. Belayev, M. Schadt, M. I. Barnik, J. Funfschilling, N. V. Malimoneko, and K. Schmitt, "Large aperture polarized light source and novel liquid crystal display operating modes," Jpn. J. Appl. Phys. **29**(4), L634–L637 (1990).
21. Y. Huang, Y. Zhou, and S. T. Wu, "Broadband circular polarizer using stacked chiral polymer films," Opt. Express **15**(10), 6414–6419 (2007).
22. A. Borbély, A. Sámson, and J. Schanda, "The concept of correlated colour temperature revisited," Color Res. Appl. **26**(6), 450–457 (2001).
23. T. W. Murphy, Jr., "Maximum spectral luminous efficacy of white light," J. Appl. Phys. **111**(10), 104909 (2012).
24. D. A. Steigerwald, J. C. Bhat, D. Collins, R. M. Fletcher, M. O. Holcomb, M. J. Ludowise, P. S. Martin, and S. L. Rudaz, "Illumination with solid state lighting technology," IEEE J. Sel. Top. Quantum Electron. **8**(2), 310–320 (2002).
25. Y. Ohno, "Color Rendering and Luminous Efficacy of White LED Spectra," Proc. SPIE **5530**, 88–98 (2004).
26. M. Schadt and W. Helfrich, "Voltage-dependent optical activity of a twisted nematic liquid crystal," Appl. Phys. Lett. **18**(4), 127–128 (1971).

1. Introduction

Lately, solid-state lighting (SSL) has been gradually replacing the incandescent light bulbs because of its higher energy efficiency, reduced heat generation and longer life time. With the invention of high performance blue light-emitting diode (LED) [1–3], phosphor-converted white LED (pc-WLED) has found widespread applications. Nowadays, the concept of smart SSL is intriguing for next generation lighting technology [4, 5], where real-time spectrum tuning is particularly essential. The adjustment of spectrum will result in different correlated color temperature (CCT), which enables *smart* tuning of the white light in terms of variable environments, such as different weathers, daytime, and temperatures, or according to multifarious situations, say, working, dining, and sporting. The importance of controlling CCT is related to the profound impact of human activity and even health in presence of background illumination. Studies show that human's visual comfort, glare, and brightness perception are indispensable to CCT [6]. Therefore, a decent CCT-tuning WLED is highly desirable.

Recently, several approaches have been proposed to fulfill this demand [7–14]. Plethora of studies concentrate on mixing different types of LEDs, such as red, green, blue (RGB) LEDs, with different ratios by driving them independently [7–9]. However, the complexities in optical and electrical components, and high cost limit their applications. Some others devote to quantum dot (QD) related CCT-tuning LED which shows good performance [10, 11], but the tradeoffs are high operation voltage and still complex configuration [15–17]. Among them, tunable color filters enabled CCT-tuning is a strong contender due to the simple device configuration, simple driving scheme, low voltage and low cost [13, 14]. Although a closely resembled Planckian locus can be achieved in dichroic-dye type tunable color filter, the CCT tuning range is limited by the dichroic ratio [13]. On the other hand, the cholesteric-film type tunable color filter can only control the transmittance of one color. As a result, it requires special LED and the tuning path is deviated from blackbody locus [14].

To solve these issues, in this paper, we propose a CCT-tunable WLED using a tunable color filter, which possesses the abovementioned advantages. More interestingly, by stacking different types of cholesteric LC films, a larger blue/yellow ratio can be achieved while maintaining close to Planckian locus.

2. Working principles and device configuration

CCT is the temperature of a given stimulus whose perceived color most closely resembles that of a Planckian radiator. Thus, the CCT is inevitably related to the spectral power distribution (SPD) of the stimulus itself. As the temperature of a Planckian radiator increases,

a larger portion of short wavelengths (blue) is expected. Thus, through dynamically tuning the blue/yellow ratio of a white light, various CCT can be achieved.

In light of this principle, we demonstrate an active color filter to produce blue and yellow complementary colors. Figure 1 depicts the schematic of our device configuration. The proposed tunable color filter consists of four passive cholesteric liquid crystal (CLC) films and an active polarization rotator, which is also a LC device.

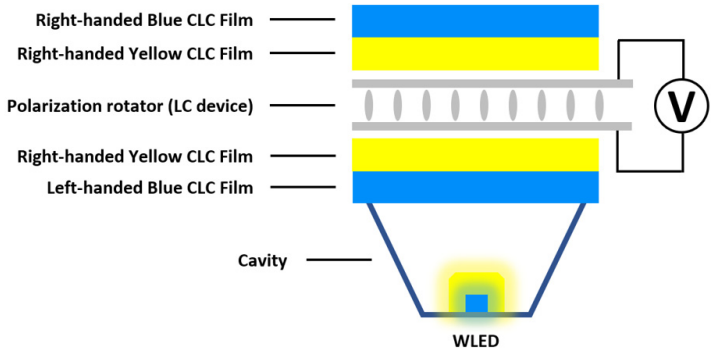

Fig. 1. Schematic of the proposed CCT-tunable WLED using a tunable color filter. The only active device is the polarization rotator.

A CLC can be formulated by doping a small concentration of chiral compound to a rod-like nematic host. In a CLC cell, the LC directors rotate continuously along the stacking direction, and a helical structure perpendicular to the layer planes is established [18, 19]. Due to the periodic helical structure, Bragg reflection of a certain circularly polarized light, depending on the handedness of the helix, is established. The pitch length of the helix (p), central wavelength (λ_0) and reflection bandwidth ($\Delta\lambda$) can be determined by:

$$p = \frac{1}{HTP \cdot c}, \tag{1}$$

$$\lambda_0 = \langle n \rangle \cdot p = \frac{n_e + n_o}{2} \cdot p, \tag{2}$$

$$\Delta\lambda = \Delta n \cdot p = (n_e - n_o) \cdot p, \tag{3}$$

where HTP is the helix twisting power of the chiral dopant, c the concentration of the chiral dopant in weight percentage, $<n>$ the average refractive index of LC host, n_e the extraordinary refractive index, n_o the ordinary refractive index, and Δn the LC birefringence.

From Eqs. (1)-(3), the CLC films can be designed by controlling the ratio between the chiral dopant and the LC host [20]. In our device, the four CLC films are stacked from bottom to top, in sequence of left-handed blue CLC, right-handed yellow CLC, right-handed yellow CLC and right-handed blue CLC. The polarization rotator is sandwiched between two yellow CLC films. The unpolarized white light emitted by the WLED will have right-handed blue light and left-handed yellow light after passing through the first two CLC films laminated on the cavity. Here it is noticed that the reflected circularly polarized light will turn to the opposite handedness after reflecting upon the cavity, leading to recycle of the light and maintaining high efficiency. When the polarization rotator, which in our proof-of-principle experiment is a VA cell, does not affect the polarization of light passing through it (say, V = 0 in Fig. 1), the light passing through the other two CLC films will have low transmittance for blue but high transmittance for yellow, resulting in a low CCT. Meanwhile, high CCT can be

Optics EXPRESS

achieved by setting the polarization rotator to be a half-wave plate for yellow, in which the left-handed yellow light will turn to right-handed and be blocked by the second right-handed yellow CLC film, while blue light would pass through the second blue CLC film. Therefore, by utilizing both circular polarizations, complementary blue and yellow colors are generated. A larger tuning range is expected because of the enlarged blue/yellow ratio, while the CCT in between these two limits can be realized by tuning the phase retardation of the polarization rotator. One trade-off of our approach is that the color filter is not an emissive type, that means it will always block some of the light, leading to a somewhat lower optical efficiency than the WLED itself.

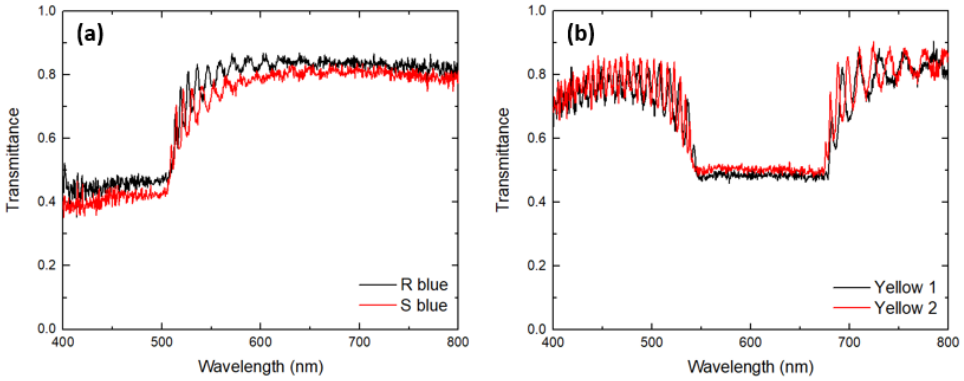

Fig. 2. Measured spectral transmittance of (a) two blue CLC films with opposite handedness, and (b) two yellow CLC films with the same handedness.

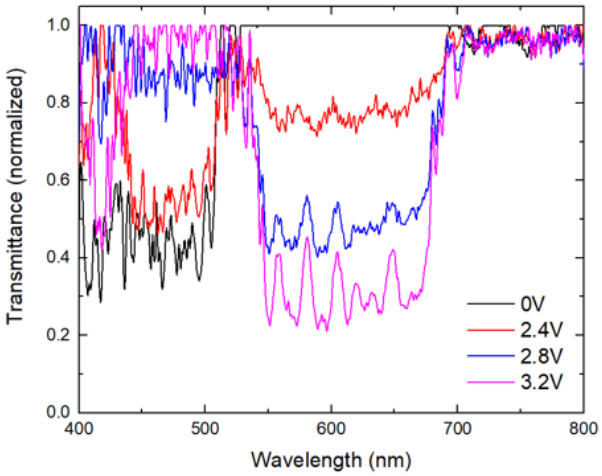

Fig. 3. Measured transmission spectra (normalized) of the tunable color filter at different voltages.

3. Experimental results

In experiment, we chose R5011 and S5011 (HCCH, China) as chiral dopants and LCM2018 (Δn = 0.44 at λ = 632.8 nm, LC Matter, USA) as LC host. These two chiral dopants have the same helical twisting power but opposite handedness. To fabricate two blue CLC cells with opposite handedness, two mixtures consisting of 3.53 wt% R5011, 96.47 wt% LCM2018 and 3.58 wt% S5011, 96.42 wt% LCM 2018 were filled into two commercial homogeneous cells with cell gap d = 5 μm, respectively. For the two yellow CLC cells with the same handedness

Optics EXPRESS

we filled a mixture consisting of 2.64 wt% R5011, 97.36 wt% LCM 2018 into the same type of cells as mentioned above. The measured transmission spectra are illustrated in Fig. 2. It is noteworthy that CLC cells were used in our proof-of-principle experiment, but in practical applications, CLC films should be utilized in order to reduce device thickness and weight [21].

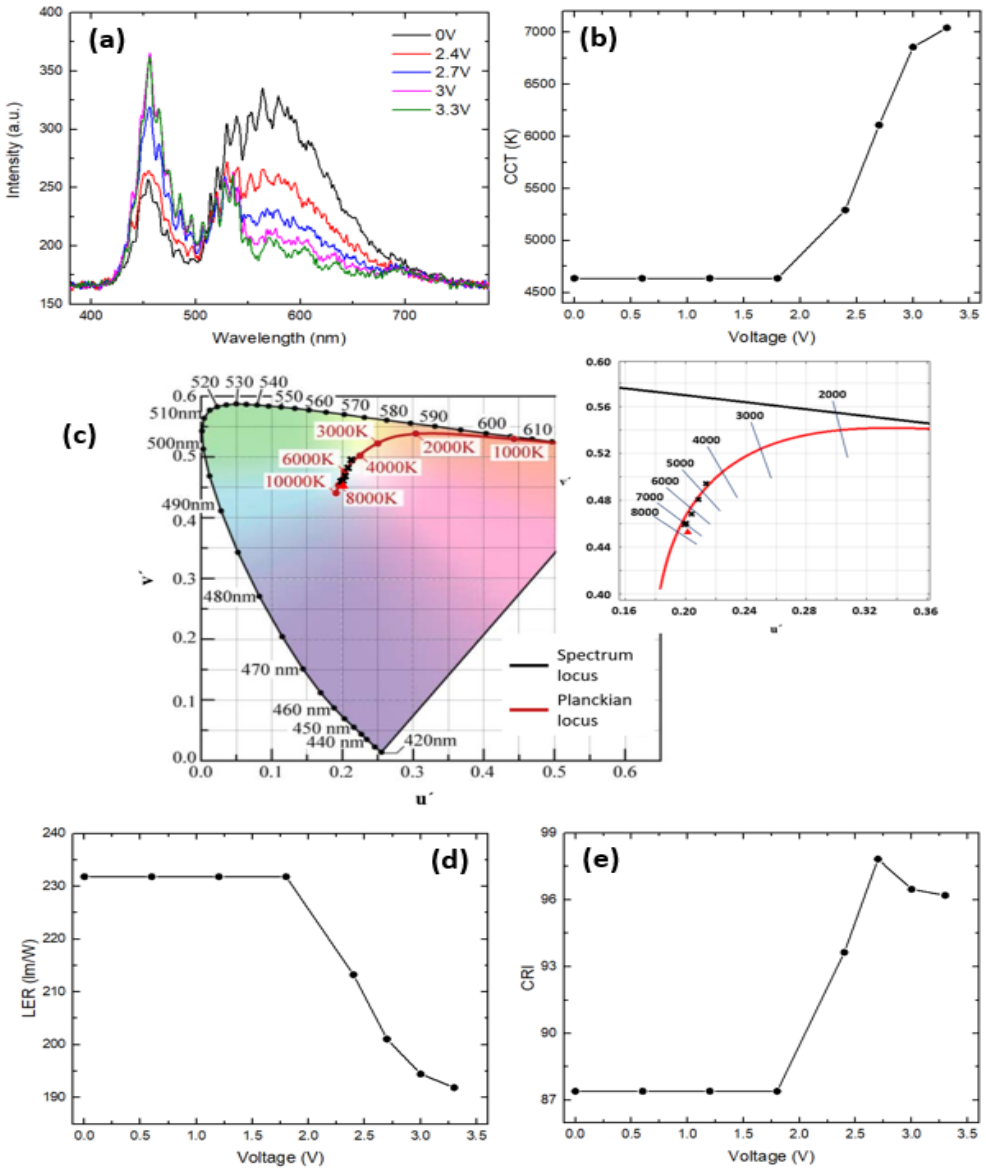

Fig. 4. (a) Measured transmission spectra and (b) corresponding CCT of WLED #1 under different voltages. (c) CCT tuning path (black crosses) in CIE 1976 color space (CIELUV) where the red triangle denotes the light source point without the tunable color filter. (a) Measured light efficacy of radiation and (b) color rendering index of WLED #1 under different voltages.

As for the polarization rotator, which is an active VA cell in our case, we filled a negative Δε (dielectric anisotropy) LC into a VA cell with cell gap d = 5 μm. The inner surface of the

substrates was over-coated with a thin indium tin oxide (ITO) electrode. Together with four fabricated CLC test cells, the tunable color filter was finally accomplished.

Figure 3 shows the normalized transmission spectra, recorded by HR2000 CG-UV-NIR high-resolution spectrometer (Ocean Optics), of this color filter under different voltages. As Fig. 3 shows, the complementary blue and yellow colors are produced using this color filter. As the applied voltage increases, the blue/yellow ratio increases. This ratio reaches its maximum at V≈3.3 V_{rms}, where the VA cell acts as a half-wave plate for yellow light. However, since our VA cell is not broadband, it is not a perfect half-wave plate for blue light, resulting in reduced transmittance in blue light as well as variation of transmittance for all wavelengths within the Bragg stop bands. Details will be discussed later.

To test the performance of adapting this tunable color filter into applicable WLEDs, we recorded the voltage-dependent spectra using two commercial WLEDs as light sources. For convenience, we mark them as WLED #1 and #2, where WLED #1 has a higher CCT than WLED #2. The measured results are depicted in Fig. 4 and Fig. 5, respectively.

The function of our tunable color filter is demonstrated in Fig. 4(a) and Fig. 5(a). Similar to Fig. 3, at low voltages, blue light has low transmittance while yellow light can pass through the color filter. As the voltage increases, yellow light starts to be partially blocked while blue light gains transmittance. At V≈3.3 V_{rms}, the VA cell works as a half-wave plate for yellow light, leading to the highest blue/yellow ratio, i.e., highest CCT. Please note that the VA cell is the only active device in our proposed tunable color filter. The required voltage is quite low, which enables an ultra-low power consumption. Moreover, the LCD technology is quite mature, which implies that such a voltage-dependent CCT can be controlled with high precision.

Figures 4(b) and 5(b) illustrate the CCT change as a function of applied voltage. The VA cell has a threshold voltage near 1.8 V. Above the threshold, LC molecules start to reorient and introduce phase retardation between two linear polarizations, leading to polarization changes. As a result, WLED #1 shows CCT tuning from ~4600 K to ~7000 K, while WLED #2 tunes the CCT from ~3000 K to ~4900 K.

Figures 4(c) and 5(c) demonstrate another way of visualizing the device performance, which shows the chromaticity in CIE 1976 color space (CIELUV). As Fig. 4(c) shows, it is intriguing that after tailoring the spectra by the color filter, the light source #1 can closely resemble the Planckian locus. Similar effect also happens to WLED #2, at some voltages. To evaluate how closely the tuning path follows the Planckian locus, we calculate the deviation (*Duv*) using the *u′*, *2/3·v′* coordinate system [22]. Our results indicate that the *Duv* is less than 0.005 for WLED #1 and less than 0.015 for WLED #2, for all measured points. The average *Duv* is 0.002 for WLED #1 and 0.011 for WLED #2. Such a small deviation for WLED #1 is quite acceptable for practical applications which demands $Duv < 0.005$, but additional effort is needed for WLED #2 to reduce the deviation [23, 24]. If we can tailor the employed light source to be closer to Planckian locus initially, then the deviation can be further minimized.

Apart from CCT, for general lighting, other parameters should be taken into consideration as well, such as luminous efficacy of radiation (LER) and color rendering index (CRI) [23, 25]. Figures 4(d-e) and 5(d-e) illustrate the voltage-dependent LER and CRI for these two CCT tunable light sources, respectively. Similar to Figs. 4(b) and 5(b), there is a threshold voltage due to the employed VA cell. As the applied voltage increases, the LER has a trend of decreasing. It can be interpreted from the tunable SPD as shown in Figs. 4(a) and 5(a). Since human eyes are more sensitive to yellow, as the voltage increases, the intensity of blue light increases and that of the yellow light decreases, leading to a decreased LER. On the other hand, CRI keeps increasing when V< 3 V_{rms}. Again, this can be explained by looking at the SPD. As the voltage increases, the spectral power is more evenly distributed on RGB, leading to a better rendering of object. As the voltage exceeds 3 V_{rms}, the CRI starts to decrease due to the decreased yellow/blue ratio. As noted from Figs. 4(e) and 5(e), the CRI of WLED #1 is

Optics EXPRESS

above 87 at all time, while WLED #2 has a lower CRI at low voltages. This index, however, can be boosted if a better blue/yellow ratio is available for the WLED itself.

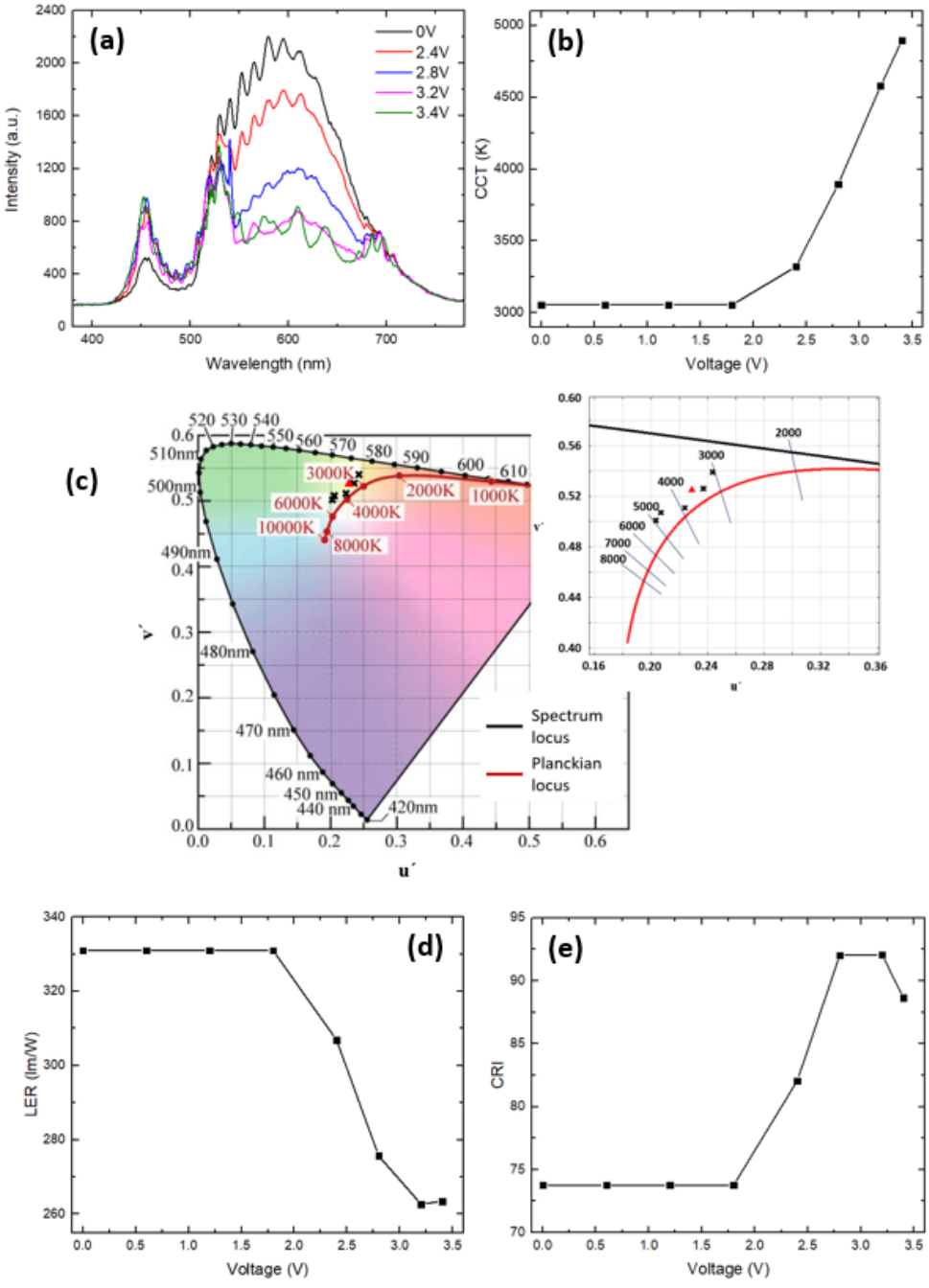

Fig. 5. (a) Measured transmission spectra and (b) corresponding CCT of WLED #2 under different voltages. (c) CCT tuning path (black crosses) in CIE 1976 color space (CIELUV) where the red triangle denotes the light source point without the tunable color filter. (d) Measured light efficacy of radiation and (b) color rendering index of WLED #2 under different voltages.

Optics EXPRESS

4. Discussion

4.1 Polarization rotator

In our proof-of-concept experiment, VA cell is used as the polarization rotator. However, in principle, other LC modes such as homogeneous cell and twisted nematic (TN) cell can also be used.

As mentioned above, VA cell is not a broadband device. One solution is to use a TN cell, which is known as a broadband half-wave plate [26]. To apply TN cell, a broadband quarter-wave plate is needed to convert the incident circularly polarized light into linear because TN mode prefers linear polarization. After the TN cell, another broadband quarter-wave plate may also be needed for higher blue/yellow ratio. Also, in this case, the off-state now has the highest blue/yellow ratio, i.e. highest CCT, while on-state stands for the lowest CCT. It is noteworthy that another advantage of using TN cell is that it offers a wider viewing angle, comparing to VA cell.

4.2 Cavity effect

In our experiment, there is no back mirror employed, meaning that approximately half of the blue and yellow lights is wasted. Yet in real device, this lost part can be recycled back into the system. This not only influences the efficiency of the device, but also has impact on maximum blue/yellow and yellow/blue ratios. It is noticed that the enlarged ratios will increase the CCT tuning range as well.

4.3 Two-WLED system

It is interesting that our experiment demonstrates two WLEDs with tuning ranges from ~3000 K to ~4900 K and from ~4600 K to ~7000 K, respectively. If we integrate, for example, these two WLEDs, into one cavity and apply the tunable color filter to this system, a wider tuning range can be achieved. In this two-WLED system, it is not necessary to dynamically tune the ratio between these two WLEDs, but only on-off control is needed. For instance, if a CCT in the range of ~3000 K to ~4800 K is required, we can switch WLED #2 on and turn WLED #1 off, while adjusting the voltage of the polarization rotator correctly.

5. Conclusion

A CCT-tunable WLED with a tunable color filter is proposed and proof-of-concept experiment is conducted. This tunable color filter consists of four passive cholesteric films and an active polarization rotator. By utilizing both circular polarizations of light, complementary colors are generated, which in our case is blue and yellow. The blue/yellow ratio can be dynamically adjusted, and the tuning range of the blue/yellow ratio is relatively large. In experiment, CCT-tuning ranges about 1900 K and 2400 K are obtained for two different commercial WLEDs and the color performance is evaluated. More interestingly, tuning path resembling Planckian locus is realized. Our approach has potential for next generation smart SSL lighting applications.

Funding

Air Force Office of Scientific Research (AFOSR) (FA9550-14-1-0279).